30th EPS Conference on Contr. Fusion and Plasma Phys., St. Petersburg, 7-11 July 2003 ECA Vol. **27A**, P-1.135

Analysis of the power deposition in the ASDEX Upgrade divertor during disruptions.

G. Pautasso, A. Herrmann, T. Eich, J.C. Fuchs, O. Gruber. A. Kallenbach and the ASDEX Upgrade Team, Max-Planck-Institut für Plasmaphysik, EURATOM Association, 85748 Garching, Germany

Introduction.

The power balance during disruptions in ASDEX Upgrade has been analized since the beginning of operation. The general picture of the power deposition mechanism in the Divertor I Phase (flat target plates) was as follows. The power density deposition profiles have always been so wide as to cover the whole divertor surface. During the thermal quench phase of the disruption up to 100 % of the thermal energy of the plasma was deposited onto the divertor plates within a few ms. In the successive current quench most of the magnetic energy associated with the plasma current was ohmically dissipated within the plasma and typically 30 % of it was found on the divertor plates. The majority of the disruptions in that experimental phase were density limits at relatively moderate plasma current (0.6-0.8 MA) and large q_{95} (4-6).

With the installation of the Divertor II-lyra and II-b and the exploration of new plasmas regimes (lower q_{95}, higher energy) the picture of power deposition has become more complex. In several discharges the thermal quench is relatively slow and the thermal energy starts leaking out of the plasma a few ms before the negative voltage spike. The power deposition profiles have remained very wide, spreading on the whole divertor surface and also outside of it (see Fig. 1).

Aim of this work is to check the power balance during recent disruptions and analyse the power deposition on the lower divertor plates from a statistical point of view.

Diagnostics.

Two IR thermography cameras, sensible to radiation with a 4.7 μm wavelength, measure the photon emission from the lower divertor plates. The power deposition profiles are then inferred from these raw data on the basis of a physical model. The two cameras are located at two different toroidal positions and observe not-overlapping poloidal regions of the divertor. The time resolution of the thermography data are in the range 0.12-1 ms; the spatial resolution is between 1 and 2 mm.

Radiation is measured by 100 bolometers mounted in 7 cameras around the plasma, which allow the reconstruction of the radiated power profile within and outside of the plasma separatrix. The time resolution of the bolometers is 1 ms.

The database.

The database, build for this work, contains 44 discharges (most of the disruptions with vertical displacement towards the bottom of the machine) with complete measurements of the power deposition on the lower divertor plates in the shot range 13000-17500 (Jan.2000 - Mai.2003). The plasma parameters of the discharges varies in the following ranges: plasma current = 0.6-1 MA, q_{95} = 2.5-6, thermal energy before disruption = 50-500 kJ, poloidal magnetic energy 0.7-1.8 MJ, time interval between the thermal quench and the end of the current quench = 10-30 ms. The 30 discharges with number $<$ 14200 pertain to the Divertor II-lyra configuration; the later 14 ones to the Diveror II-b geometry. The database contains disruptions with different causes; the differentiated

discussion of the power balance for several disruption types is not yet aim of this paper.

Phenomenology.

The thermal energy of the plasma before disruption is in average much smaller (20 %) than the maximum thermal energy reached by the plasma during the discharge. The way the energy content of the plasma degrades before thermal quench varies: a large fraction of the energy may be lost during one or more minor disruptions, or it may continuously degrade within 10-100 ms.

The disruption consists of two phases: (1) the thermal quench, lasting a few ms, in which most of the plasma thermal energy is conducted along the scrape-off-layer to plasma facing components (wall or divertor); (2) the current quench, in which the electric current is dissipated by the enhanced resistivity of the cold plasma.

The energy may start leaking out of the plasma a few ms before thermal quench making the thermal quench itself a slow phenomenon lasting several ms. The parametric dependence of these different behaviors cannot be pointed out definitively yet. In any case the power deposition on the divertor plates during the thermal quench is not limited to a few 100s μs but lasts 2-3 ms in ASDEX Upgrade. The time of the thermal quench is chosen at the minimum (or center) of the negative voltage spike and has an accuracy of $\pm$ 0.5 ms.

By visual inspection of a large number of time histories of the spatially integrated power, we find that there is no one typical time history but a variety of them. The power density profiles are very broad and extend outside of the divertor region; details of the profile of energy deposition are discussed further in the paper.

Energy balance.

The *plasma before disruption* is carrier of thermal (E_{th}) and poloidal magnetic energy, $E_{mag} = 0.5\, I_p^2\, \mu\, R\, ln(\frac{8R}{a\sqrt{k}} - 2 + \frac{l_i}{2})$ associated with its toroidal electric current. At the end of the current quench the pre-disruptive plasma energy can be found as thermal energy on the plasma facing components (conducted and convected, E_{con}, or deposited by radiation, E_{rad}), and as electromagnetic energy - i.e. current - in electric conductors (E_{em}) coupled by mutual induction to the plasma. During the whole disruption, auxiliary heating is on and keeps inputing energy (E_{in}) into the plasma.

The energy balance equation for the plasma can be written as:

$$\Delta E_{mag} + \Delta E_{th} + \Delta E_{in} = \Delta E_{con} + \Delta E_{rad} + \Delta E_{em} \qquad (1)$$

The energy balance can be applied to any time interval during the discharge. The different terms of the above equation have been computed for a variety of discharges both in the steady state phase and in disruptions. As an example, we discuss here the energy balance of a disruption after density limit (shot n. 13540) for the thermal quench and current quench phases separately. Time traces of several plasma parameters during the disruption are shown in Fig. 2. The energy in the following table is expressed in MJ.

phase.	ΔE_{mag}	ΔE_{th}	ΔE_{in}	$\Delta E_{div} - \Delta E_{div_{rad}} = \Delta E_{con}$	ΔE_{rad}	ΔE_{em}
th. qu.	> 0	0.16	~ 0	< 0.15	0.13	~ 0
whole	$\simeq 1.0$	0.16	0.08	0.5-0.4 = 0.1	0.7	0.15

The term E_{con} is the difference between the energy observed on the divertor plates by the thermography (E_{div}) and the energy deposited on the divertor plates by radiation ($E_{div_{rad}}$) and calculated from the radiation profiles, reconstructed from the bolometer. The energy balance over the whole disruption is within 30 % of the original energy content correct.

Energy onto the divertor plates.

The amount of energy deposited onto the divertor plates may change from disruption to disruption. Therefore it is necessary to look at the statistical distribution of the power deposited onto divertor and its different parts. The database described above is used for this analysis.

The amount of energy deposited on the lower divertor during the whole disruption is in average 30 % (and can reach 45 %) of the total pre disruptive energy of the plasma ($E_{tot} = E_{th} + E_{mag}$). During the 4 ms centered about the thermal quench time, the energy deposited on the lower divertor is in average 90 % (and can reach 200 %) of the thermal energy. This suggests that during this time already a fraction of the magnetic energy is dissipated.

A statistical evaluation of the amount of energy deposited onto the different parts of the divertor is reported in the following table for the discharges of the Divertor II-lyra configuration. For this purpose the divertor has been subdivided in 8 regions as shown in Fig. 3. The table reports the amount of energy deposited on the divertor plate during the whole disruption (E_{div}) and during the 4 ms about the thermal quench (E^{th}_{div}) relative to E_{tot} and ($E_{th} + 0.1E_{mag}$) respectively; σ is the standard deviation of the distribution of these quantities for 30 discharges. S_n is the area of each divertor region.

Region n.	1	2	3	4	5	6	7	8
$E_{div(n)}/E_{tot}$ %		4.0	1.4	3.6	4.4	2.1	4.8	6.6
σ		2.2	0.4	1.0	1.1	0.8	2.5	1.7
$E^{th.qu.}_{div(n)}/(E_{th} + 0.1E_{mag})$ %		10.0	2.2	4.6	5.3	2.6	10.6	8.8
σ		6.0	0.7	1.7	2.2	1.3	6.6	3.0
S_n (m^2)	2.13	1.29	0.69	0.90	1.15	0.97	1.79	2.22

The thermography measurements on region n. 1 are not correct and therefore disregarded. (In the whole paper $E_{div} = \sum_n E_{div(n)}$, where $E_{div(n)}$ is the energy deposited on the nth region and $E_{div(1)}$ is assumed equal to $E_{div(8)}$.) We conclude that the *strike point modules* (regions n. 2 and 7) are more loaded than the other part of the divertor during the thermal quench and that the energy is nearly uniformly distributed during the current quench. These results are illustrated in Fig. 4, where the mean of the amount of energy per unit surface has been plotted in an histogram for the different divertor regions and disruption phases. Similar results are obtained for the divertor II-b.

Future work.

Further work of analysis is underway to determine: the influence (1) of the disruption type, (2) of plasma parameters on the power deposition pattern and (3) the limits of the accuracy of the energy and power balance due to the error bars on the measurements. (4) The influence of the divertor geometry will be further assessed by comparing disrupted plasmas moving downwards with the ones moving upwards.

Acknowledgments. We acknowledge usefull discussions with A. Loarte and G. Federici.

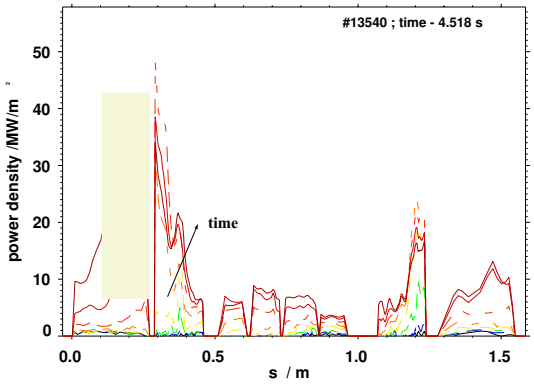

Figure 1. Time evolution of the power deposition profiles on the lower divertor plates during the thermal quench. The profiles are 0.12 ms apart.

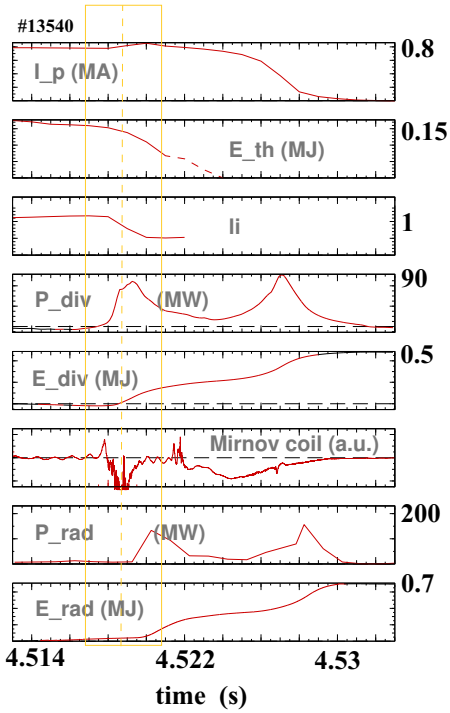

Figure 2. (on the right) Time histories of several plasma parameters during disruption. I_p is the plasma current, E_{th} is the thermal energy, li is the internal inductance, P_{div} and E_{div} are the power and energy deposited on the divertor plates, P_{rad} and E_{rad} are the power and energy radiated.

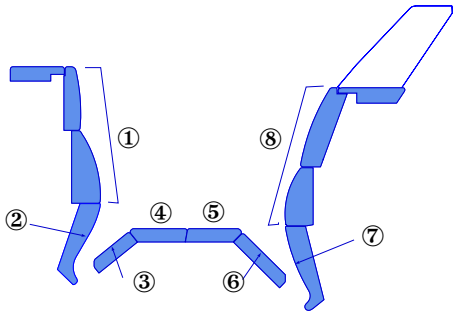

Figure 3. Divertor II-lyra geometry and its 8 regions.

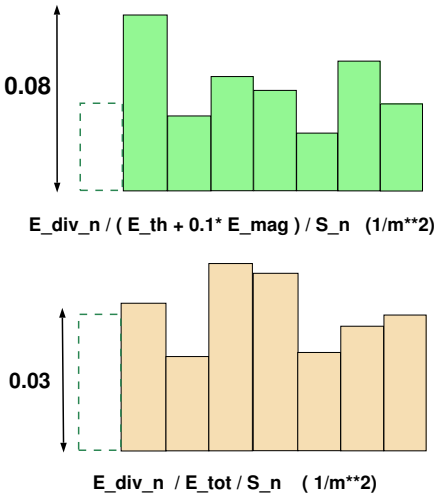

Figure 4. (on the right) Histogram of the energy per unit surface deposited on the different divertor regions (30 disruptions) during the thermal quench phase **(upper)** and whole disruption **(lower).**